Reduced-Order Modeling of Composite Floor Slabs in Fire. II: Thermal-Structural Analysis

Jian Jiang[1]; Joseph A. Main, M.ASCE[2]; Jonathan M. Weigand, A.M.ASCE[3]; and Fahim Sadek, M.ASCE[4]

Abstract: This paper describes a reduced-order modeling approach for the thermal and structural analysis of fire effects on composite slabs with profiled steel decking. The reduced-order modeling approach, which uses alternating strips of layered shell elements to represent the thick and thin portions of the slab, allows both thermal and structural analyses to be performed using a single model. The modeling approach accounts for: (1) the trapezoidal profile of the concrete in the ribs; (2) the structural resistance provided by the steel decking, including the webs of the decking; and (3) the orthotropic behavior of the decking, which provides greater resistance along the ribs than transverse to the ribs. The modeling approach is validated against experimental data from one-way composite slabs tested under ambient-temperature, a one-way composite slab tested under fire conditions, and a two-way composite slab tested under fire conditions. Both implicit and explicit solution schemes are evaluated for the structural analysis, and the results show that it is feasible to scale down the hours-long fire duration to a simulation time of seconds in an explicit dynamic analysis, without adversely affecting the accuracy of the results. The steel decking contributes significantly to the structural resistance at an ambient temperature, but as expected, its contribution is found to decrease rapidly under fire exposure. The modeling approach can account for the location of reinforcing bars (i.e., at a specified depth in either the thick or thin portion of the slab), and it is found that reinforcement location can have a significant effect on the structural response, because heat transfer in the composite slab results in higher temperatures in the thin portions of the slab between the ribs. **DOI: 10.1061/(ASCE)ST.1943-541X.0002607.**

Author keywords: Thermal-structural analysis; Composite slab; Reduced-order model; Shell element; Validation; Explicit analysis.

Introduction

Typical composite floor slabs used in modern steel-framed buildings consist of concrete topping on profiled steel decking. Analyzing the response of composite slabs to fire loading requires both thermal analysis, as discussed in the companion paper (Jiang et al., forthcoming), and structural analysis, which is the focus of this paper. Temperature distributions obtained from thermal analysis influence the structural response through thermal expansion and through degradation of material stiffness and strength. As discussed in the companion paper (Jiang et al., forthcoming), the types of models commonly used for structural analysis of composite slabs are generally not suitable for thermal analysis. In previous structural analyses of composite slabs under fire loading (e.g., Lamont et al. 2004; Lim et al. 2004; Foster et al. 2007; Yu et al. 2008), temperature histories in the slab have been prescribed within the structural analysis model, and the suitability of the modeling approach for thermal analysis was not considered. A key objective of this study is to develop a reduced-order modeling approach for composite slabs that is suitable for both thermal and structural analyses. Allowing the same model to be used for both types of analyses facilitates evaluation of the response of large structural systems under various fire scenarios.

Challenges in the structural analysis of composite slabs exposed to fire include properly accounting for the orthotropic behavior associated with the ribbed profile (i.e., differences in stiffness parallel and perpendicular to the ribs) and properly capturing the effects of material and geometric nonlinearities at large deformations. A number of different numerical modeling approaches have been developed for the structural analysis of composite slabs under fire conditions (e.g., Elghazouli et al. 2000; Huang et al. 2001; Lamont et al. 2004; Izzuddin et al. 2004; Jiang and Usmani 2013). Three-dimensional (3D), high-fidelity finite-element models, in which the concrete is modeled with solid elements and the profiled decking is modeled with shell elements (Both 1998; Sadek et al. 2008; Alashker et al. 2010), can realistically simulate the orthotropic behavior of composite slabs, as well as material and geometric nonlinearities. However, such high-fidelity models require significant computing time, making them impractical for the analysis of large structural systems. Therefore, many researchers have attempted to develop reduced-order modeling approaches for composite slabs that use beam and/or shell elements. These approaches are discussed in the subsequent paragraphs.

The simplest modeling approach employs a grillage of beam elements to approximate the response of a composite slab (Elghazouli et al. 2000; Elghazouli and Izzuddin 2000; Sanad et al. 2000). In this grillage approach, T-section beams span in the direction of the ribs, representing the combination of the ribs and the continuous upper

[1]Research Structural Engineer, Engineering Laboratory, National Institute of Standards and Technology, 100 Bureau Dr., Mail Stop 8611, Gaithersburg, MD 20899-8611.

[2]Research Structural Engineer, Engineering Laboratory, National Institute of Standards and Technology, 100 Bureau Dr., Mail Stop 8611, Gaithersburg, MD 20899-8611.

[3]Research Structural Engineer, Engineering Laboratory, National Institute of Standards and Technology, 100 Bureau Dr., Mail Stop 8611, Gaithersburg, MD 20899-8611 (corresponding author). ORCID: https://orcid.org/0000-0002-6938-6197. Email: jonathan.weigand@nist.gov; jweigand@uw.edu

[4]Research Structural Engineer, Engineering Laboratory, National Institute of Standards and Technology, 100 Bureau Dr., Mail Stop 8611, Gaithersburg, MD 20899-8611.

Note. This manuscript was submitted on April 24, 2019; approved on October 15, 2019; published online on March 19, 2020. Discussion period open until August 19, 2020; separate discussions must be submitted for individual papers. This paper is part of the ***Journal of Structural Engineering***, © ASCE, ISSN 0733-9445.

portion of the slab (above the decking), and flat rectangular beams span in the transverse direction, representing the continuous upper portion of the slab (above the decking). Results using this approach showed that the influence of the ribs was significant and should be included in the analysis. The disadvantage of the grillage approach is its inability to properly simulate tensile membrane action, which can develop in conjunction with a ring of compressive forces around the supported edges of a deflecting slab.

To enable modeling of membrane action in composite slabs, Huang et al. (2000) and Izzuddin et al. (2004) developed modified shell-element formulations that account for the orthotropic properties of composite slabs. Huang et al. (2000) applied an effective stiffness factor to modify the material stiffness matrices of plain concrete, allowing shell elements with uniform thickness to represent the orthotropic behavior of a composite slab. Izzuddin et al. (2004) introduced a flat shell element for ribbed composite slabs that considered geometric and material nonlinearities and incorporated two additional displacement fields corresponding to stretching and shearing modes in the rib region, thus indirectly accounting for the effect of the rib on the membrane and bending actions transverse to the rib orientation. Both of these approaches use shell elements with the same thickness and material properties to represent the orthotropic properties of a composite slab. A limitation of this approach is that differences in thermal effects on the thick and thin portions of the slab cannot be captured. These differences can be significant for composite slabs exposed to fire, because the thin portions heat more quickly than the thick portions, and thus experience more significant degradation in stiffness and strength.

Rather than attempting to use a single type of shell elements to represent the orthotropic properties of a composite slab, Lim et al. (2004) proposed a hybrid approach in which shell elements were used to represent the continuous upper portion of the slab (above the decking) and beam elements were used to represent the ribs. Using a similar approach, Yu et al. (2008) developed an orthotropic slab element assembled from a layered plate element representing the continuous concrete slab and a beam element representing a group of ribs.

More recently, Kwasniewski (2010) and Main (2014) proposed approaches in which alternating strips of layered shell elements were used to represent the thick and thin portions of a composite slab. Verification of these modeling approaches was presented through comparisons with high-fidelity finite-element analyses.

The studies by Kwasniewski (2010) and Main (2014) were limited to ambient temperature. However, the suitability of using alternating strips of shell elements for thermal analysis of composite slabs has been demonstrated in the companion paper (Jiang et al., forthcoming). Jiang et al. (forthcoming) presented a reduced-order modeling approach for thermal analysis that consisted of alternating strips of layered composite shell elements to represent the thick and thin portions of the composite slab, with appropriate approximations to account for the effects of the profiled decking and ribs. Comparisons with experimental measurements demonstrated that this approach could accurately capture heat transfer in composite slabs exposed to fire. This paper presents the development and application of the same type of reduced-order modeling approach for structural analysis of composite slabs subjected to fire effects. While of higher fidelity than the grillage-type approach described previously, the proposed approach is designated as reduced-order in comparison to detailed modeling approaches that use solid elements. A key advantage of the proposed approach is the ability to use a single, consistent modeling approach for both the thermal and structural analysis.

In this study, the reduced-order modeling approach was implemented for both separate and coupled thermal-structural analysis of composite floor slabs. The separate thermal and structural analyses presented in this paper involved detailed thermal models with an implicit numerical scheme and reduced-order structural models with an explicit numerical solver. The coupled thermal-structural analyses used reduced-order thermal models with an implicit numerical formulation and reduced-order structural models with an implicit solver incorporating automatic implicit-explicit switching, when needed, to achieve global convergence. The reduced-order modeling approach consisted of alternating strips of layered shell elements, representing the thick and thin portions of the slab. Key issues for the development of the reduced model are discussed, including evaluating the contribution of the webs of the decking and the tapered profile of concrete in the ribs on the load-bearing capacity. Validation of the reduced-order modeling approach is then presented through comparison with experimental results from a one-way slab at an ambient temperature, a one-way slab at elevated temperatures, and a two-way slab at elevated temperatures. Two different analysis approaches were used for the model validation: separate thermal and structural analyses and coupled thermal-structural analysis. The effects of temperature distribution, reinforcement location, and profiled rib geometry on the behavior of composite slabs in fire were studied. Further details on the thermal analysis of composite slabs using high-fidelity and reduced-order models can be found in Jiang et al. (2017).

Reduced-Order Modeling Approach

Fig. 1 illustrates the proposed reduced-order modeling approach for thermal and structural analyses of composite slabs. The modeling approach is described in the following subsections, which address the composite shell representation, the material modeling, and the numerical solution schemes. The analyses presented in this study were performed using the LS-DYNA finite-element software (LSTC 2014).

Composite Shell Representation

The proposed reduced-order modeling approach uses a layered composite shell formulation (*PART_COMPOSITE in LS-DYNA), in which the thickness of each layer is specified, along with a distinct structural material and thermal material. This allows individual layers to be specified for the steel decking and the reinforcement, with multiple layers representing concrete through the thickness of the slab. As illustrated in Fig. 1, the proposed approach uses alternating strips of shell elements to represent the thick portion (Shell A) and thin portion (Shell B) of a composite slab. The width of the thick and thin portions of the slab can each be spanned by a single shell element or by multiple shell elements, depending on the required mesh refinement, as discussed subsequently.

While the upper and lower flanges of the steel decking can be modeled as layers in the composite shell approach (Fig. 1), the webs of the decking cannot be modeled directly. To account for the structural resistance provided by the webs of the decking, half of the cross-sectional area of each web is assigned to the upper flange, the other half is assigned to the lower flange, and the thicknesses of the upper and lower flanges are increased accordingly. Letting l_0 and l_3 denote the widths of the web and the upper flange, respectively (Fig. 1), the thickness of the upper flange is thus increased to $t_d(1 + l_0/l_3)$, where t_d is the actual thickness of the decking. Similarly, the thickness of the lower flange is increased to $t_d(l_2/l_1 + l_0/l_1)$, where the first term in parentheses is less than unity because the width of Shell A (total width at the top of the rib), l_1, is larger than the width of the lower flange, l_2 (Fig. 1).

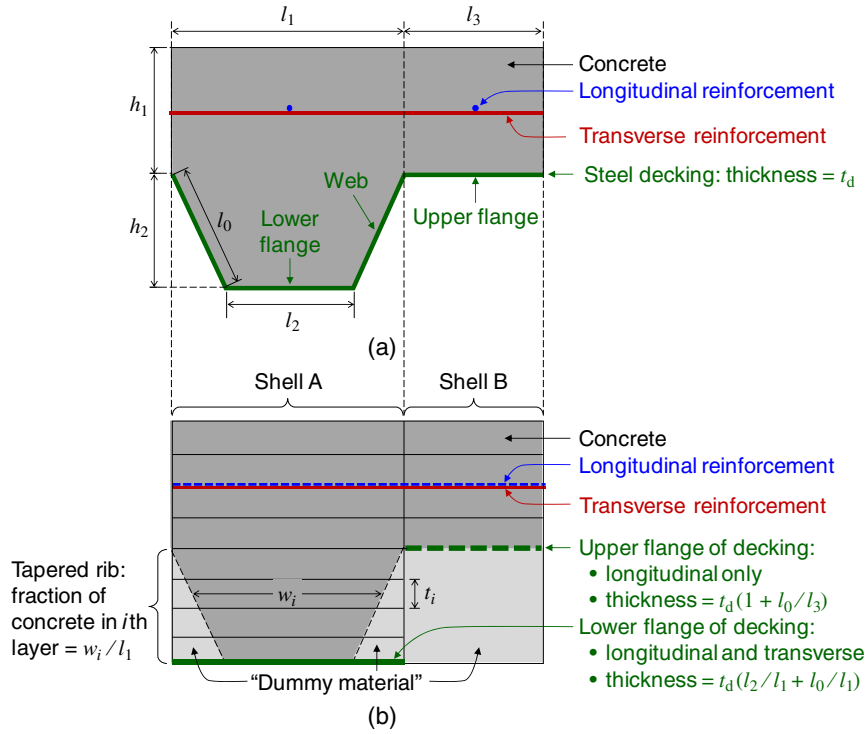

Fig. 1. Illustration of reduced-order modeling approach: (a) geometry of concrete slab on profiled steel decking; and (b) layered composite shell representation.

The profiled steel decking provides much greater resistance along the ribs than transverse to the ribs, since the ribs can unfold like an accordion under transverse loading. To account for this behavior, the upper flange of the decking in Shell B is specified to provide no resistance to transverse loading. This is achieved by using a concrete material model that allows different values of the reinforcement ratio along perpendicular axes (material 172 in LS-DYNA; see section on time scaling), and by specifying negligible strength for the concrete, with zero reinforcement ratio transverse to the ribs and a reinforcement ratio of unity (pure steel) parallel to the ribs.

The tapered profile of concrete in the ribs is represented by specifying the fraction of concrete in the ith layer (by cross-sectional area) to be w_i/l_1, where w_i is the average rib width for the ith layer [Fig. 1(b)]. The remaining fraction of cross-sectional area in the ith layer is specified to have negligible strength and stiffness. This is achieved by using a concrete material model that allows a fraction of each layer to be specified as reinforcement (material 172 in LS-DYNA; see section on time scaling), and by specifying very low values of strength and stiffness for the reinforcement, so that it functions as a dummy material with negligible structural resistance. The fraction of the ith layer assigned to the dummy material is then given by $(1 - w_i/l_1)$.

It should be noted that the composite shell formulation used in the reduced-order modeling approach assumes the composite behavior of all layers and thus does not allow for the possibility of debonding of the steel decking from the concrete slab. Such debonding can occur as a result of differential thermal expansion and temperature-induced degradation in strength of the fire-exposed decking relative to the somewhat cooler concrete slab. The extent of such debonding, and its effect on the load-bearing capacity of the slab, depend not only on the fire exposure, but also on the detailing of the profiled decking, which typically incorporates stiffeners and embossments that promote bonding with the concrete. If debonding of the decking is localized (e.g., if debonding of the lower flange occurs but the webs remain bonded), then composite action between the concrete and the steel decking may be largely maintained. Widespread debonding, however, could result in a loss of composite action. Within the reduced-order composite shell approach, the effect of debonding could potentially be modeled by reducing the strength and stiffness of the decking when the temperature exceeds a specified debonding temperature. However, the appropriate debonding temperature for a specific type of decking would need to be evaluated. In this study, debonding is not considered, and composite action is assumed to be maintained between the decking and the concrete slab. Comparisons of analysis results with experimental data provide confirmation that the assumption of composite behavior was appropriate for the cases considered in this study, even though local debonding of the bottom flange of the decking was noted in one of the experiments.

Material Modeling

For structural material characterization, the material MAT_172 (MAT_CONCRETE_EC2) was used, where the stress-strain curves for concrete and steel at ambient and elevated temperatures are based on the Eurocode EC2 [EN 1992-1-2 (CEN 2005)]. These curves for concrete and steel at ambient temperatures are shown in Fig. 2, scaled to the user-defined compressive strength and tensile strength of concrete, and modulus of elasticity and yield strength of reinforcement. The temperature dependence of the stress-strain relationship and thermal expansion coefficients are taken from EC2. Future work will include implementing more accurate temperature-dependent stress-strain relationships, particularly for steel, based on recent work at NIST (Seif et al. 2016). The material model (MAT_172) was used to model concrete, steel decking, and embedded steel reinforcement.

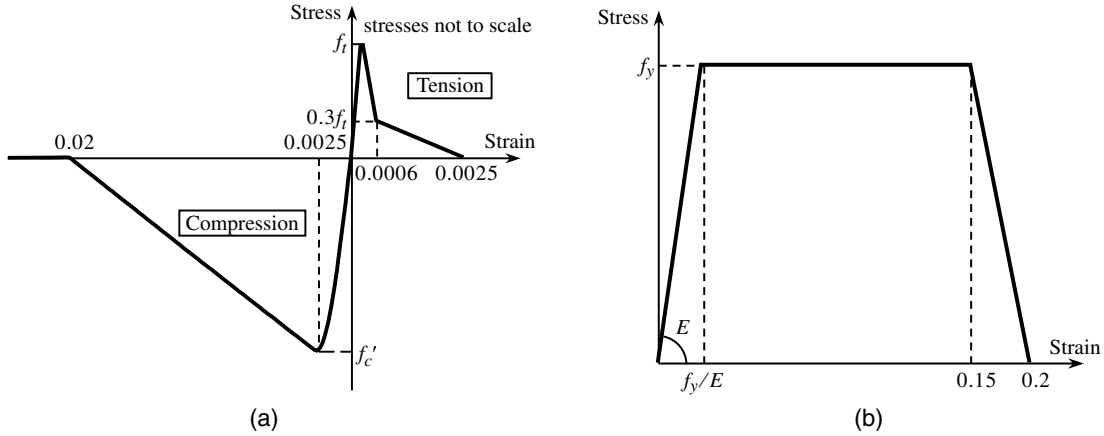

Fig. 2. Stress-strain relationships used in modeling: (a) concrete; and (b) steel.

For modeling plain concrete only, a reinforcement ratio of zero was used, while for metal decking only, a reinforcement ratio of unity was implemented. A reinforcement ratio between zero and unity was used for modeling reinforced concrete with evenly distributed reinforcement.

Numerical Solution Schemes

To capture the structural response of slabs at large displacements and elevated temperatures, dynamic time-history analyses were performed in this study. Time integration methods for solving the dynamic equilibrium equations are broadly categorized as either explicit or implicit. The primary difference between these two integration schemes lies in their determination of the responses at time $t + \Delta t$ based on the results at time t alone for explicit analysis, and at time $t + \Delta t$ for implicit analysis. As a result, implicit analysis methods require an iterative solution process for each time step. The avoidance of iterations in explicit analysis is at the expense of requiring very small time steps, typically on the order of $10^{-5} \sim 10^{-6}$ s, to ensure a stable and accurate solution. The requirement of small time steps in explicit analysis can result in a significant computational burden for analysis of large structural systems and/or long-duration responses. Implicit integration schemes allow for larger time steps, but can encounter convergence problems as the structure undergoes some type of failure (e.g., buckling or fracture) or experiences softening or loss of stiffness. For an hours-long structure-fire analysis, implicit time integration would typically be used, while for analysis of structural response to a subsecond-duration blast pulse, explicit time integration would generally be more effective. However, for highly nonlinear problems, smaller time steps may also be required in implicit analyses to meet convergence requirements, or convergence may fail altogether. Thus, the selection of the most appropriate solution scheme may vary from case to case.

In this study, for the separate thermal and structural analyses of composite slabs, an implicit solver was used in the thermal analysis while an explicit solver was used for the structural analysis. To reduce the computational cost, the hours-long heating duration was scaled down to a time period of a few seconds in the structural analysis. For the coupled thermal-structural analysis, the analysis used an implicit solver by default, but automatically switched to an explicit solver for structural analysis when needed to overcome convergence problems. Using this approach, no time scaling is needed.

In the next three sections, the modeling approach described in the preceding paragraph is validated against experimental data from one-way composite slabs tested at an ambient temperature, a one-way slab tested under fire conditions, and a two-way composite slab tested under fire conditions. The validation under fire loading includes both separate and coupled thermal-structural analyses. As indicated earlier, separate thermal and structural analyses include high-fidelity thermal models and reduced-order structural models. The high-fidelity thermal models used were developed and validated in an earlier study (Jiang et al. 2017). The high-fidelity thermal models are used for the separate thermal and structural analyses because they provide slightly better accuracy than the reduced-order thermal models. The coupled thermal-structural analyses use the reduced-order modeling approach for both thermal and structural analysis, thus providing validation of the reduced-order modeling approach for both types of analysis.

One-Way Slab at Ambient Temperature

Three structural tests at ambient temperatures were carried out on simply supported one-way composite slabs by Baskar and Antony Jeyasehar (2012), with the geometry shown in Fig. 3. Embossments were used in the decking sheet, and the ends of the tested slabs were anchored by shear studs to prevent slippage between the concrete slab and steel deck. This is typical in practice, and also consistent with the assumption in the reduced-order structural model of no slippage between the concrete slab and decking. The slab had a

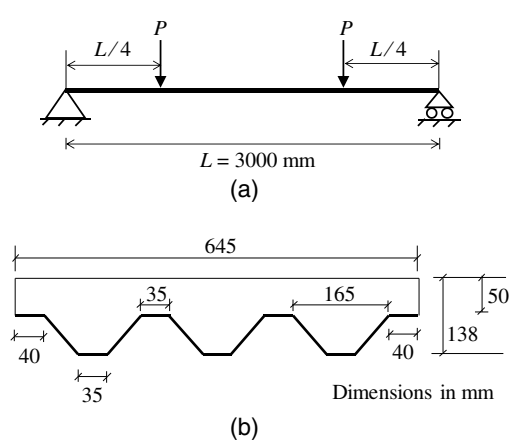

Fig. 3. One-way slab test at ambient temperature: (a) schematic; and (b) cross section. (Data from Baskar and Antony Jeyasehar 2012.)

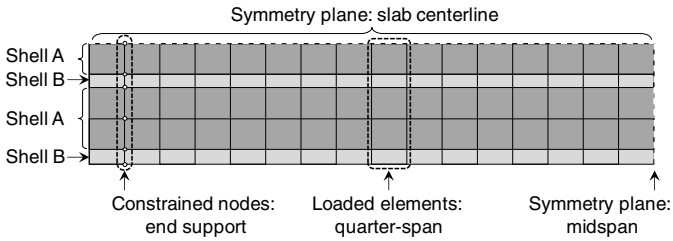

Fig. 4. Reduced-order model of one-way slab test (quarter of slab).

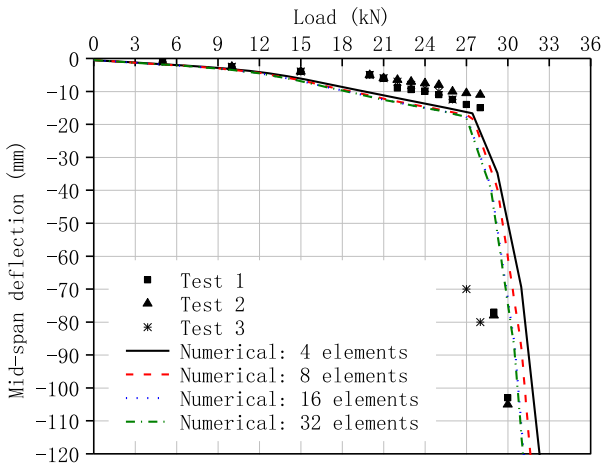

Fig. 5. Comparison of load versus mid-span deflections from experiments and from reduced models with different mesh sizes.

span of 3.0 m and a width of 0.645 m. No reinforcing bars were used, and the 0.8-mm-thick steel decking acted as the reinforcement. The mean compressive strength of concrete was 55 MPa. The modulus of elasticity and yield strength of the steel decking were 200 GPa and 375 MPa, respectively. Loads were gradually applied at two quarter-span points ($L/4$) with hydraulic jacks until failure of the slab was observed. The tested slabs had an average ultimate load of $2P = 29$ kN.

Mesh Sensitivity

Due to symmetry, only one quarter of the slab was included in the reduced-order model, as illustrated in Fig. 4. Mesh sensitivity analysis was carried out with mesh densities ranging from 4 elements to 32 elements along the half-length of the slab. The results of the mesh sensitivity analysis along with the experimental results are shown in Fig. 5. The results were fairly insensitive to the mesh size. The mesh size with 16 elements was used for the subsequent analyses. The results in Fig. 5 show that the model accurately captured the ultimate load (within 5% of the experimental data) with a sharp increase in deflections at failure, consistent with the experiments. The model slightly underestimated the initial stiffness compared with the experiments in the load range of 0–15 kN. For applied loads larger than 15 kN, the underestimation of the stiffness became more significant (by about 13%–54%).

Contribution of Decking Web and Concrete Rib

A parametric study was conducted to understand the influence of the webs of the steel decking and the tapered profile of the concrete in the ribs on the structural behavior of the slab. For that purpose,

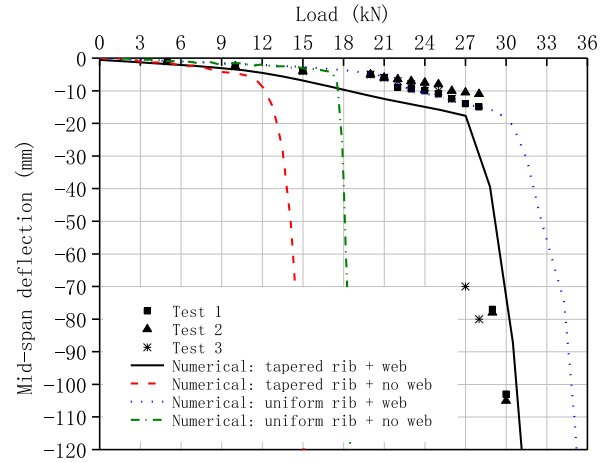

Fig. 6. Comparison of load versus midspan deflections between test and numerical analysis for the contribution of web.

Fig. 6 shows the results of four different analyses: (1) an analysis that includes the webs of the decking and accounts for the tapered profile of concrete in the ribs, as presented in the previous section (same results as shown in Fig. 5); (2) an analysis that accounts for the tapered profile of concrete in the ribs but includes no contribution from the webs of the steel decking; (3) an analysis that includes the webs of the decking but represents the concrete in the ribs as having a uniform width of l_1; and (4) an analysis that includes no contribution from the webs of the steel decking and represents the concrete in the ribs as having uniform width.

Fig. 6 shows that representing the concrete in the rib as having uniform width, instead of the realistic tapered profile, resulted in a decrease in the midspan deflection of the slab because the amount of concrete in the rib was overestimated. For the cases without decking, accounting for the tapered profile resulted in a noticeable decrease in the load-bearing capacity of the slab (relative to the analysis with uniform rib width), because the tensile resistance in flexure was provided by the concrete alone. On the other hand, for the cases with decking, accounting for the tapered profile had a less significant effect due to the presence of the decking, which provides tensile reinforcement in flexure. Neglecting the decking webs would reduce the load-bearing capacity of the slab by approximately 60% (from 27.5 to 10.5 kN). These results show the importance of properly modeling the tapered ribs and the webs of the decking for composite slabs at an ambient temperature.

At elevated temperatures, the influence of steel decking (lower flange, web, and upper flange) on the overall strength of the slab is often ignored as the decking is subjected to high temperature (SCI 1991). This approach might be adequate for slabs that are acting compositely with the floor beams because the slab including the steel decking is primarily in compression under gravity loads. However, that is not the case for the simply supported slabs considered in this study where the bottom of the slab including the steel decking is in tension under gravity loading, especially for unreinforced slabs, where the steel decking might be the only member to carry that tension.

One-Way Slab at Elevated Temperature

A standard fire test on a simply supported one-way composite slab (Hamerlinck et al. 1990), denoted as Test 2, was selected to validate the proposed reduced-order structural modeling approach at elevated temperatures. Fig. 7 shows the geometry of the tested slab.

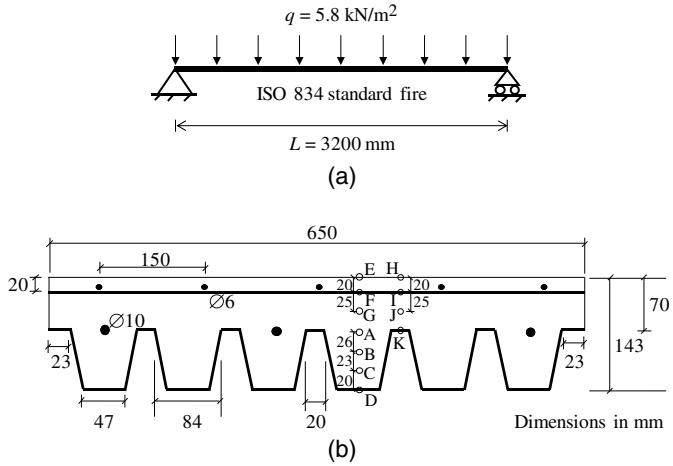

Fig. 7. One-way slab test at elevated temperature: (a) schematic; and (b) cross section. (Data from Hamerlinck et al. 1990.)

The slab had a span of 3.2 m and a width of 0.65 m. The slab consisted of Prins PSV73 steel decking with a thickness of 0.75 mm and normal weight concrete with a measured moisture content of 3.4%. The compressive strength of concrete was 25 MPa. The yield strength was 552 MPa for the 6-mm diameter reinforcing bars that were placed 20 mm below the top of the slab and 587 MPa for the 10-mm diameter reinforcing bars that were placed at the top of selected ribs. The yield strength of the steel decking was 280 MPa. The slab was subjected to a uniformly distributed load of $q = 5.8\ \mathrm{kN/m^2}$ (dead load $= 2.8\ \mathrm{kN/m^2}$; live load $= 3\ \mathrm{kN/m^2}$) that was kept constant for 2 h during the ISO 834 (ISO 2014) standard fire.

The subsequent sections deal with separate thermal and structural analyses of the composite slab, as well as the coupled thermal-structural analysis. In both approaches, the reduced-order modeling approach described in previous sections was used for the structural analysis of the composite slab. Because of the symmetry of the test setup, only one-quarter of the slab was modeled, using a similar approach, as was illustrated previously in Fig. 4. Gravity loading was first applied at an ambient temperature, and the gravity loading was then held constant throughout the duration of the fire.

Heat Transfer Analysis

A heat transfer analysis for this test was previously conducted by Jiang et al. (2017) using a high-fidelity finite-element model, and Fig. 8 compares the numerically computed temperatures with measured temperatures at the points labeled in Fig. 7(b). In addition to the single-point temperatures, Fig. 8 also presents average temperatures at the height of each labeled point, which were calculated by averaging the numerically computed temperatures across the width of the thick and thin portions of the slab. The predicted single-point temperatures agreed well with the test data (within 5%, see Jiang et al. 2017). Because of the temperature gradient across the width of the rib, which resulted from heat input through the fire-exposed webs of the decking (Jiang et al. 2017), the average temperature in the thick portion of the slab was generally somewhat larger than the single-point temperature at the center of the rib (by as much as 25%). The influence of this temperature gradient on the structural responses is discussed in subsequent sections.

Structural Analysis

In the separate thermal and structural analyses approach, the structural analysis was performed using the reduced-order composite shell modeling approach, and temperature histories for each layer in each composite shell element were prescribed based on the computed temperatures from the high-fidelity thermal analysis. The average temperature for each layer in a composite shell element was obtained by averaging the computed temperatures at the corresponding height in the high-fidelity thermal model, over a width corresponding to the composite shell element. Explicit time integration was used for the structural analysis, with a time-scaling technique to reduce the required computational time. The sensitivity of the structural response to mesh size and the sensitivity to the time scale factor are also discussed in subsequent sections.

Mesh Sensitivity

A spanwise mesh sensitivity analysis was conducted for mesh densities ranging from 2 elements to 16 elements per half-span of the slab, and the computed time histories of midspan deflection for each mesh density are shown in Fig. 9. For the structural analyses presented in Fig. 9, the temperature time-histories from Fig. 8 were used, with the duration of 2 h (7,200 s) scaled down to 14.4 s, which was found to be a sufficiently slow loading rate to avoid introducing spurious dynamic effects in the response. The widths of the thick and thin portions of the slab were each spanned by a single shell element, as shown in Fig. 10(a). The results show that the midspan deflection was fairly insensitive to the mesh size along the span. A mesh of eight elements per half-span was used in the subsequent analyses, and for this mesh refinement, the difference between the measured and computed deflections did not exceed 18%.

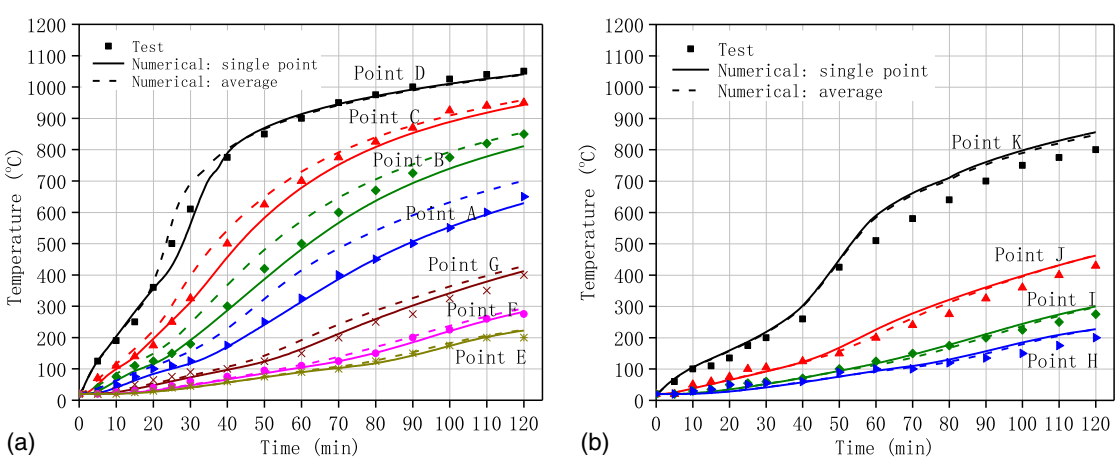

Fig. 8. Comparison of measured and calculated temperatures in the slab: (a) thick part; and (b) thin part.

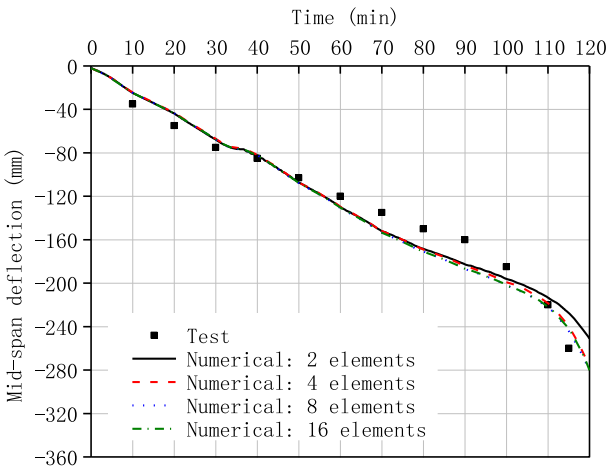

Fig. 9. Comparison of midspan deflections for different mesh sizes.

Additional analyses were performed to evaluate the sensitivity of the computed results to the number of elements across the width of the thick and thin portions of the slab, as illustrated in Fig. 10. When representing the thick and thin parts of a composite slab using only one element each [i.e., the coarse mesh shown in Fig. 10(a)], each layer of the composite shell is assigned a temperature obtained by averaging the nodal temperatures at that height from the high-fidelity thermal model across the entire width illustrated in Fig. 10(a). The coarse mesh thus does not capture horizontal temperature gradients across the width of the rib, which can be significant, as evidenced by the differences between the single-point temperatures and the average layer temperatures in Fig. 8. To better capture these temperature gradients, additional elements were used across the width of the thick and thin portions of the slab, as illustrated for the medium mesh in Fig. 10(b) and the fine mesh in Fig. 10(c), and the prescribed layer temperatures were averaged over these reduced widths. As shown in Fig. 11, the midspan deflections of the heated slab were fairly insensitive to the horizontal mesh refinement. This indicates that local deviations from the average temperature had a relatively small effect on the total flexural capacity, which results from integration of all the layer forces over the cross section. For the subsequent analyses, the coarse mesh in Fig. 10(a) was used.

Time Scaling

Because only static structural responses are considered in this study, time can be artificially scaled in the structural analysis without affecting the solution, provided that the loads and the temperature variations are applied sufficiently slowly that spurious dynamic effects are not introduced. When using explicit time integration for the structural analysis, reducing the duration of the analysis through a time-scaling technique can significantly reduce the required computational time. In analyzing the one-way slab at elevated temperatures, different time scale factors were considered, in which the temperature time-histories of 2 h (7,200 s) were scaled down to 14.4, 7.2, 2.4, and 0.6 s. The midspan deflection time histories for the various time scales are shown in Fig. 12. The reduced analysis times of 0.6 and 2.4 s resulted in more obvious oscillations in the response, indicating that dynamic effects were introduced by the rapidly applied thermal loading. The oscillation decreased as computational time increased, and no oscillation in the structural response was observed at 14.4 s corresponding to a time scale factor of $(7{,}200\ \mathrm{s})/(14.4\ \mathrm{s}) = 500$. As a result, a time scale factor of 500 was used in subsequent analyses.

Coupled Thermal-Structural Analysis

For the separate thermal and structural analyses presented previously, it was necessary to map the nodal temperatures from the high-fidelity thermal analysis to the corresponding layer temperatures in each composite shell element by averaging over the appropriate node sets, layer by layer and element by element. For analysis of a large structural system subjected to a realistic fire (e.g., with thermal loading from a fire dynamics simulation), implementation of this mapping process would impose a significant burden. There are distinct advantages to a coupled thermal-structural analysis approach, in which the same model is used for both thermal and structural analysis, and no mapping of temperatures is required. For the coupled thermal-structural analyses in this study, implicit time integration with automatic implicit-explicit switching was used for the structural analysis. If convergence of the equilibrium iterations in the implicit analysis failed, the solution automatically switched to explicit analysis for a predefined time interval. After this time interval, the solution process would switch back to implicit time integration and attempt to proceed. When using this approach, the time interval for the explicit analysis should be small enough to avoid the introduction significant dynamic effects during the explicit phase. In this study, a time interval of 0.001 s was used.

A coupled thermal-structural analysis was carried out to simulate the fire effects on the analyzed one-way slab. Fig. 13 presents a comparison of measured midspan deflection of the slab against deflections predicted using the coupled thermal-structural analysis outlined in this section and the separate thermal and structural analyses presented earlier. The figure shows some discrepancy between the separate and coupled structural analyses for the latter part of the response after about 50 min. Two factors contribute to this difference: (1) the temperature distribution where the high-fidelity thermal model was used for the separate analysis while the reduced

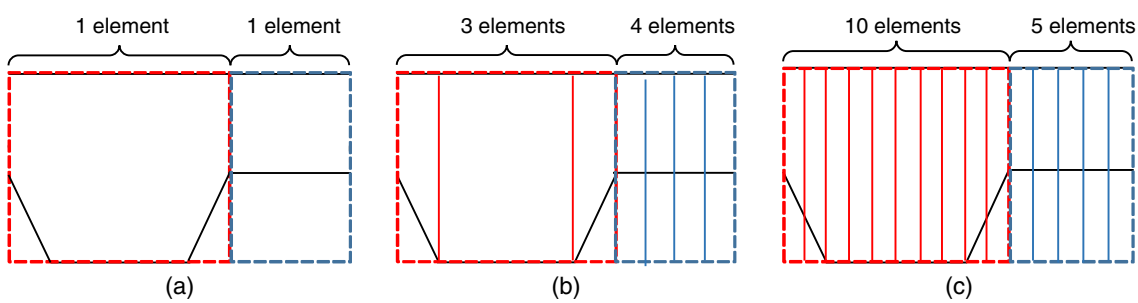

Fig. 10. Different meshes in the cross section of slabs to consider the nonuniform temperature: (a) coarse mesh; (b) medium mesh; and (c) fine mesh.

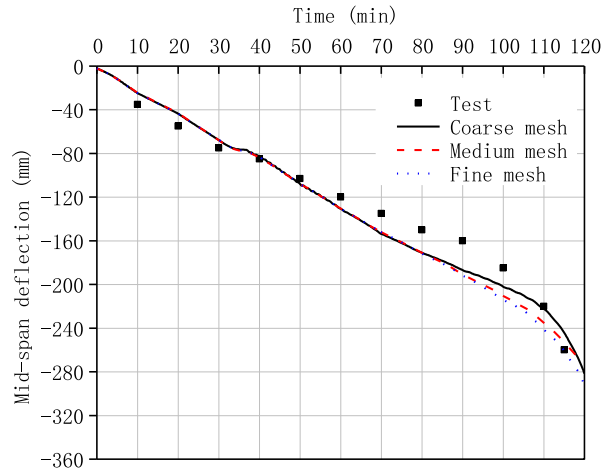

Fig. 11. Comparison of midspan deflections of slabs considering different meshes with nonuniform temperature distribution.

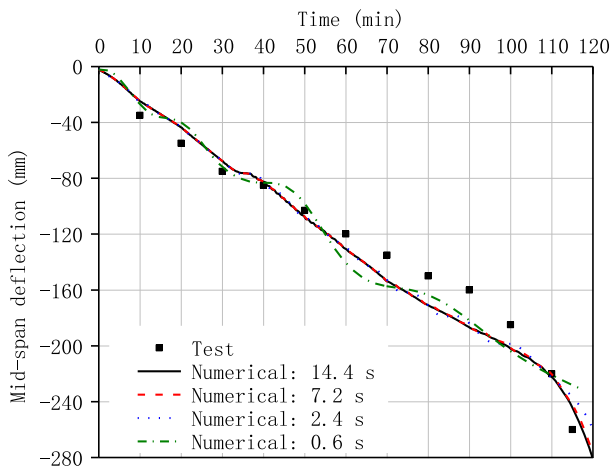

Fig. 12. Comparison of midspan deflections against different time scales.

order thermal model was used for the coupled analysis, and (2) the numerical solver where an explicit formulation was used for the separate analysis while an implicit scheme with automatic implicit-explicit switching was used for the coupled analysis. Nevertheless, Fig. 13 shows a similar failure time of about 100–110 min for both the separate and coupled analyses.

Two-Way Slab at Elevated Temperature

The thermal-structural modeling approach was again validated against the results of a two-way composite slab tested in the Building Research Association of New Zealand (BRANZ) furnace (Lim 2003). The geometry of the slab is shown in Fig. 14. The slab was simply supported on four edges and unrestrained against in-plane movements. The slab had a width of 3.15 m and a length of 4.15 m (aspect ratio = 1:1.3). The Dimond Hibond decking had a thickness of 0.75 mm and a total depth of 130 mm. Hot-rolled reinforcing bars with a diameter of 8.7 mm and spacing of 300 mm in both directions were used at a distance of 20 mm above the ribs. The yield strengths of the reinforcement and decking were 565 and 550 MPa, respectively. Siliceous aggregates were used for the

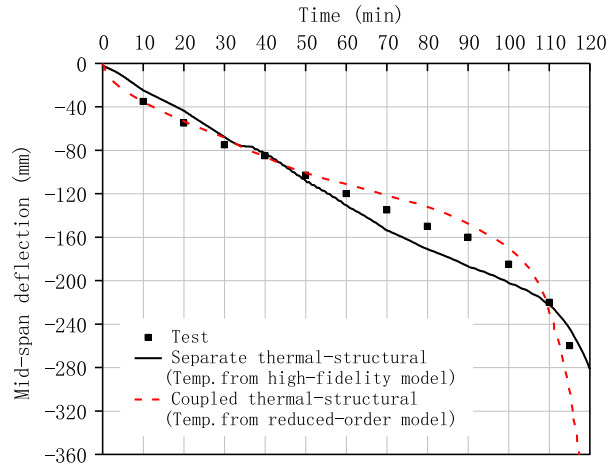

Fig. 13. Comparison of midspan deflection of the one-way slab from test, separate and coupled thermal-structural analyses.

concrete, which had a compressive strength of 32 MPa. A uniformly distributed load of 5.4 kN/m^2 (resulting in a demand-capacity ratio of 0.18) was imposed on the slab. The tested slab was exposed to the ISO 834 (ISO 2014) fire for 4 h.

Heat Transfer Analysis

Using a high-fidelity thermal model, temperatures in the slab were calculated, and a comparison of temperatures between measured and numerical results is shown in Fig. 15 (Jiang et al. 2017). The average temperatures shown in the figure were used for the subsequent structural analysis. The largest-magnitude deviation between the test and analysis results was observed at Point A at the bottom surface of the concrete slab (Fig. 14), where a maximum temperature difference of 192°C were observed, which corresponds to 10% of the temperature at the end of the test. This large temperature difference at Point A was due to debonding of the steel decking from the concrete slab that was observed in the test (Lim 2003), which disrupted the heat transfer from the steel decking to the lowermost surface of the concrete slab in the experiment, leading to lower measured temperatures [see Jiang et al. (2017) for more details].

Structural Analysis

Mesh Sensitivity and Time Scaling

A similar procedure to what was used in the preceding for the one-way slab was used herein to determine the optimum mesh size and time scaling. As a result, a mesh size of 12 elements per one quarter of the slab was used for the remainder of this section. In addition, the 4-h fire duration was scaled down to 10 s, resulting in a time scaling of $(14{,}400\ \mathrm{s})/(10\ \mathrm{s}) = 1{,}440$, which was used for the subsequent analyses. This scaling factor was found to allow a sufficiently slow thermal loading to avoid introducing spurious dynamic effects in the response.

Modeling of Decking and Reinforcement

In this section, two important modeling assumptions for two-way composite floor slabs are discussed and examined. The first assumption deals with unidirectional versus bidirectional behavior of the steel decking, and the second deals with how reinforcing bars are included in the model. The accuracy of these assumptions are investigated using computational modeling.

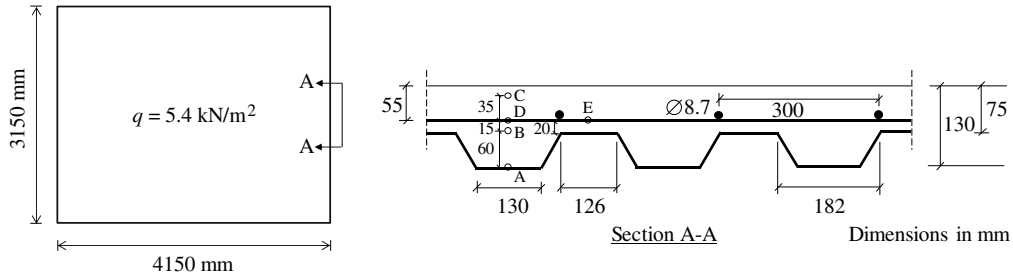

Fig. 14. Schematic of two-way slab test at elevated temperature. (Data from Lim 2003.)

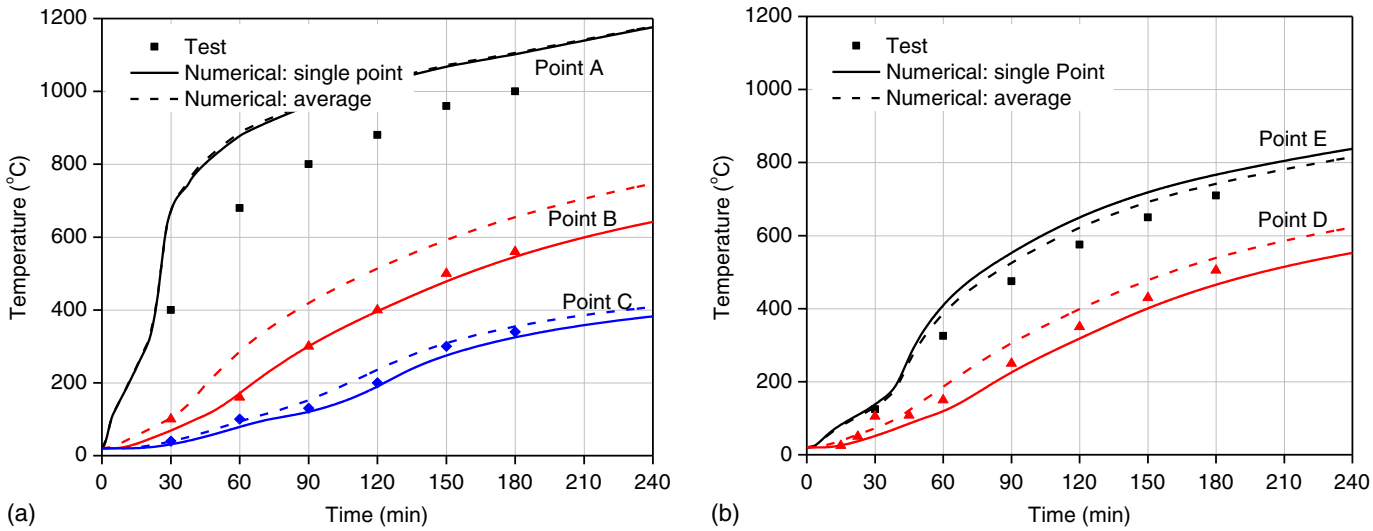

Fig. 15. Comparison of measured and calculated temperatures: (a) at the thick part; and (b) reinforcement.

Steel decking: To account for the directionality of the steel decking in the analysis, the steel decking may be modeled in two ways: bidirectional or unidirectional. Bidirectional modeling of the decking assumes that the decking is continuous both along the ribs and transverse to the ribs. As indicated in preceding sections, this assumption might not be appropriate because the steel decking provides much larger resistance along the ribs than transverse to the ribs. Unidirectional modeling of the decking, on the other hand, is more realistic because it assumes that the decking is not continuous in the direction transverse to the ribs, neglecting any forces that can be transferred by the decking in this direction. Unidirectional decking can be simulated in the numerical model by considering the top flange of the decking as orthotropic and canceling the strength of all top flanges in the transverse direction. This is graphically depicted in Fig. 16 using dashed lines at the location of the upper flange of the steel decking to represent the orthotropic top flange.

Reinforcement: In the test specimen, the reinforcement parallel to the ribs was placed in the thin portion of slab (reinforcement shown using dashed lines at the location of the longitudinal reinforcement in Fig. 16), which had a higher temperature than the reinforcement at the same height in the thick portion of slab [compare temperatures at Point E (thin portion) with Point D (thick portion) in Fig. 15]. There are two ways in which this reinforcement may be modeled: a smeared steel layer uniformly distributed in both the thick and thin portions of the slab (Shells A and B), or a smeared steel layer in the thin portion only (Shell B). The first approach means that a portion of the reinforcement is placed in the thick portion with a lower temperature compared to the test specimen. As a result, this approach might lead to a lower temperature for the reinforcing bars, and thus smaller deflections. The second approach should be more realistic because it results in a more accurate temperature in the reinforcing bars in the thin portion of the slab.

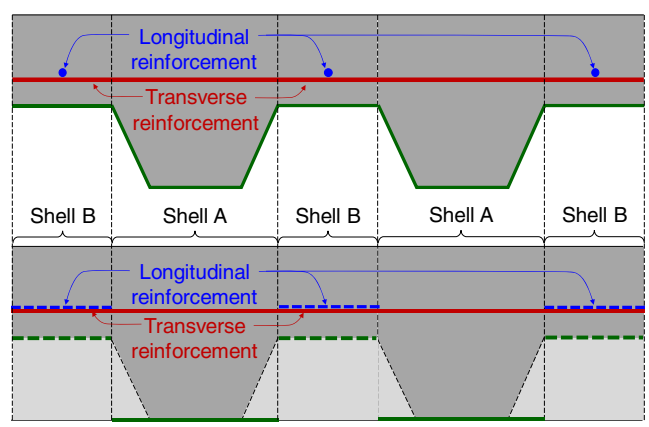

Fig. 16. Modeling of reinforcement placed in the thin portion of the slab.

Comparisons: Fig. 17 shows a comparison of the experimentally measured central deflection of the two-way composite slab with analysis results using three different models:

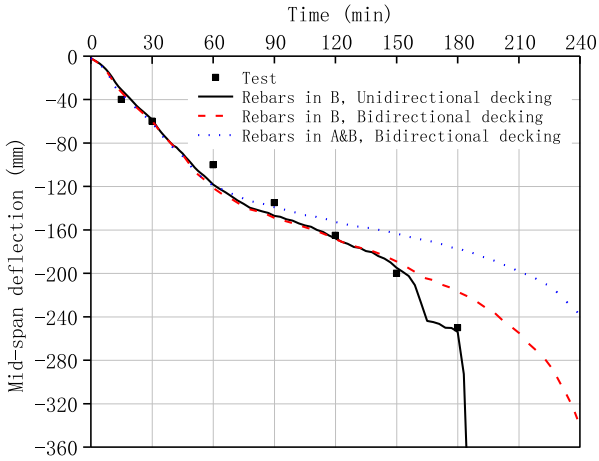

Fig. 17. Comparison of central deflection of slab considering continuity of decking and location of reinforcement.

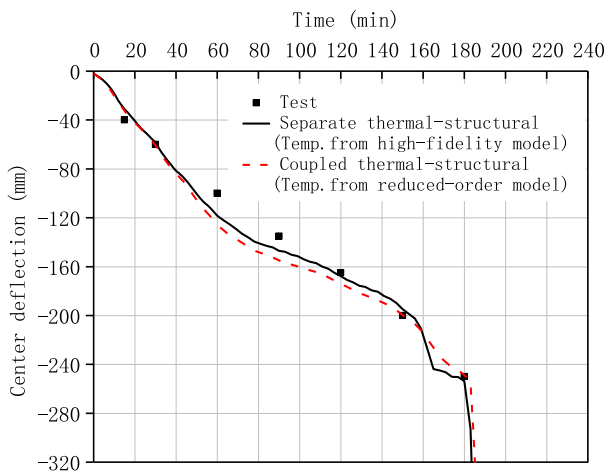

Fig. 18. Comparison of midspan deflection of BRANZ slab from test, separate, and coupled thermal-structural analyses.

- Model 1: reinforcing bars in Shell B only with unidirectional decking behavior,
- Model 2: reinforcing bars in Shell B only with bidirectional decking behavior, and
- Model 3: reinforcing bars in Shells A and B with bidirectional decking behavior.

Comparing Models 2 and 3, it is evident that the concentration of reinforcement in Shell B (model 2) produced a larger deflection at the later stages of heating than that based on Model 3 with the smeared steel layer in both the thick and thin portions of the slab (Shells A and B). This comparison also indicates that Model 2 achieved better agreement with the measured deflections.

A comparison between Models 1 and 2 indicates that, as expected, the assumption of unidirectional decking behavior results in larger deflections than the assumption of bidirectional decking. This comparison also indicates that better agreement with the experimental results is obtained with the unidirectional decking assumption with close agreement between computed and experimental midspan deflection at failure (about 180 min). In summary, the model that had reinforcing bars in Shell B only with unidirectional decking behavior (Model 1) resulted in the best agreement with the experimental results. The largest deviation of the computed deflections for this model from the measured values was 19% (at 60 min).

Coupled Thermal-Structural Analysis

A coupled thermal-structural analysis was carried out to simulate the fire effects on the two-way slab analyzed in section "Two-Way Slab at Elevated Temperature." The coupled analysis used the model that had reinforcing bars in Shell B only with unidirectional decking behavior (Model 1). Fig. 18 presents a comparison of measured central deflection of the slab against deflections predicted using the coupled and separate thermal and structural analyses. The figure shows that the responses from both analyses are very similar.

Conclusions

This paper presented the development and validation of a reduced-order modeling approach for thermal-structural analysis of composite slabs with profiled steel decking exposed to fire. Both separate and coupled thermal-structural analyses were performed and the results were compared. The following conclusions can be drawn:

1. The reduced-order modeling approach for composite slabs, using alternating strips of shell elements representing the thick and thin parts of composite slabs, was found to be suitable for both separate and coupled thermal-structural analyses. When coupled thermal-structural analysis is used, the reduced-order approach allows both thermal and structural analyses to be performed using a single model. The performance of the proposed model was validated against experimental data from one-way composite slabs tested under ambient-temperature, a one-way composite slab tested under ISO 834 (ISO 2014) standard fire conditions, and a two-way composite slab also tested under ISO 834 standard fire conditions.
2. The tapered profile of the ribs and the resistance provided by the webs of the metal decking were found to have noticeable effects on the structural behavior of composite slabs at ambient temperatures, and appropriate methods of modeling these effects were presented. The responses of composite slabs were found to be fairly insensitive to the mesh size, and thus a relatively coarse mesh could be used to reduce the computational cost.
3. The approach of smearing reinforcement in the simulation by using one layer of reinforcement across the slab section was not always suitable for composite slabs, because the temperatures of the thick and thin portions of the slab may be quite different. In the reduced-order modeling approach, the actual placement of the reinforcement can be represented by including reinforcement layers in the thick portion, the thin portion, or both, as appropriate, to better capture the temperature distribution in the reinforcement, which significantly affects the structural behavior of slabs exposed to fire.
4. It was feasible to perform structural analysis with explicit time integration to avoid the convergence problems often encountered in implicit analyses. To reduce the required computational time, a 1-h heating duration was scaled down to several seconds in the explicit dynamic analysis without introducing spurious dynamic effects. Implicit time integration with automatic implicit-explicit switching was also found to be a suitable approach to overcome convergence problems in the implicit structural analysis. This approach was implemented in the coupled thermal-structural analyses.

Disclaimer

Certain commercial entities, equipment, products, or materials are identified in this document in order to describe a procedure or concept adequately. Such identification is not intended to imply recommendation, endorsement, or implication that the entities, products, materials, or equipment are necessarily the best available for the purpose. The policy of the National Institute of Standards and Technology is to include statements of uncertainty with all NIST measurements. In this document, however, measurements of authors outside of NIST are presented, for which uncertainties were not reported and are unknown.

References

Alashker, Y., S. El-Tawil, and F. Sadek. 2010. "Progressive collapse resistance of steel-concrete composite floors." *J. Struct. Eng.* 136 (10): 1187–1196. https://doi.org/10.1061/(ASCE)ST.1943-541X.0000230.

Baskar, R., and C. Antony Jeyasehar. 2012. "Experimental and numerical studies on composite deck slabs." *Int. J. Eng. Res. Dev.* 3 (12): 22–32.

Both C. 1998. "The fire resistance of composite steel-concrete slabs." Ph.D. dissertation. Dept. of Engineering Structures, Delft Univ. of Technology.

CEN (European Committee for Standardization). 2005. *Eurocode 2 Design of concrete structures: Part 1.2: General rules, Structural fire design*, EN 1992-1-2. Brussels, Belgium: CEN.

Elghazouli, A. Y., and B. A. Izzuddin. 2000. "Response of idealised composite beam-slab systems under fire conditions" *J. Constr. Steel Res.* 56 (3): 199–224. https://doi.org/10.1016/S0143-974X(00)00006-7.

Elghazouli, A. Y., B. A. Izzuddin, and A. J. Richardson. 2000. "Numerical modelling of the structural fire behaviour of composite buildings." *Fire Saf. J.* 35 (4): 279–297. https://doi.org/10.1016/S0379-7112(00)00044-8.

Foster, S., M. Chladná, C. Hsieh, I. Burgess, and R. Plank. 2007. "Thermal and structural behaviour of a full-scale composite building subject to a severe compartment fire" *Fire Saf. J.* 42 (3): 183–199. https://doi.org/10.1016/j.firesaf.2006.07.002.

Hamerlinck, R., L. Twilt, and J. Stark. 1990. "A numerical model for fire-exposed composite steel/concrete slabs." In *Proc., 10th Int. Specialty Conf. on Cold-formed Steel Structures*, 115–130. Columbia, MO: Univ. of Missouri.

Huang, Z., I. W. Burgess, and R. J. Plank. 2000. "Effective stiffness modelling of composite concrete slabs in fire." *Eng. Struct.* 22 (9): 1133–1144. https://doi.org/10.1016/S0141-0296(99)00062-0.

Huang, Z., I. W. Burgess, and R. J. Plank. 2001. "Non-linear structural modelling of a fire test subject to high restraint." *Fire Saf. J.* 36 (8): 795–814. https://doi.org/10.1016/S0379-7112(01)00040-6.

ISO. 2014. *Fire-resistance tests–Elements of building construction*. ISO 834-11, Geneva: ISO.

Izzuddin, B. A., X. Y. Tao, and A. Y. Elghazouli. 2004. "Realistic modelling of composite and R/C floor slabs under extreme loading—Part I: Analytical method." *J. Struct. Eng.* 130 (12): 1972–1984. https://doi.org/10.1061/(ASCE)0733-9445(2004)130:12(1972).

Jiang, J., J. A. Main, F. Sadek, and J. M. Weigand. 2017. *Numerical modeling and analysis of heat transfer in composite slabs with profiled steel decking*. NIST Technical Note 1958. Gaithersburg, MD: National Institute of Standards and Technology.

Jiang, J., J. A. Main, J. M. Weigand, and F. Sadek. 2020. "Reduced-order modeling of composite floor slabs in fire. I: Heat transfer analysis." *J. Struct. Eng.* 146 (6): 04020080. https://10.1061/(ASCE)ST.1943-541X.0002650.

Jiang, J., and A. S. Usmani. 2013. "Modelling of steel frame structures in fire using OpenSees." *Comput. Struct.* 118 (Mar): 90–99. https://doi.org/10.1016/j.compstruc.2012.07.013.

Kwasniewski, L. 2010. "Nonlinear dynamic simulations of progressive collapse for a multistory building." *Eng. Struct.* 32 (5): 1223–1235. https://doi.org/10.1016/j.engstruct.2009.12.048.

Lamont, S., A. S. Usmani, and M. Gillie. 2004. "Behaviour of a small composite steel frame structure in a "long-cool" and a "short-hot" fire." *Fire Saf. J.* 39 (5): 327–357. https://doi.org/10.1016/j.firesaf.2004.01.002.

Lim L. C. S. 2003. "Membrane action in fire exposed concrete floor systems." Ph.D. dissertation. Dept. of Civil and Natural Resources Engineering, Univ. of Canterbury.

Lim, L. C. S., A. Buchanan, P. Moss, and J. M. Franssen. 2004. "Numerical modelling of two-way reinforced concrete slabs in fire." *Eng. Struct.* 26 (8): 1081–1091. https://doi.org/10.1016/j.engstruct.2004.03.009.

LSTC (Livermore Software Technology Corporation). 2014. *LS-DYNA Keyword User's manual, R7.1*. Livermore, CA: LSTC.

Main, J. A. 2014. "Composite floor systems under column loss: Collapse resistance and tie force requirements." *J. Struct. Eng.* 140 (8): A4014003. https://doi.org/10.1061/(ASCE)ST.1943-541X.0000952.

Sadek, F., S. El-Tawil, and H. S. Lew. 2008. "Robustness of composite floor systems with shear connections: Modeling, simulation, and evaluation." *J. Struct. Eng.* 134 (11): 1717–1725. https://doi.org/10.1061/(ASCE)0733-9445(2008)134:11(1717).

Sanad, A. M., S. Lamont, A. S. Usmani, and J. M. Rotter. 2000. "Structural behaviour in a fire compartment under different heating regimes—Part 1 (slab thermal gradients)." *Fire Saf. J.* 35 (2): 99–116. https://doi.org/10.1016/S0379-7112(00)00024-2.

SCI (Steel Construction Institute). 1991. *The fire resistance of composite floors with steel decking*. 2nd ed. London: SCI Publication.

Seif, M., J. A. Main, J. M. Weigand, T. P. McAllister, and W. Luecke. 2016. "Finite element modeling of structural steel component failure at elevated temperatures" *Structures* 6: 134–145. https://doi.org/10.1016/j.istruc.2016.03.002.

Yu, X. M., Z. Huang, I. W. Burgess, and R. J. Plank. 2008. "Nonlinear analysis of orthotropic composite slabs in fire." *Eng. Struct.* 30 (1): 67–80. https://doi.org/10.1016/j.engstruct.2007.02.013.